

# Mechanical buckling of functionally graded plates using a refined higher-order shear and normal deformation plate theory

A.M. Zenkour<sup>\*1,2</sup> and M.H. Aljadani<sup>1,3</sup>

<sup>1</sup>Department of Mathematics, Faculty of Science, King Abdulaziz University, Jeddah 21589, Saudi Arabia

<sup>2</sup>Department of Mathematics, Faculty of Science, Kafrelsheikh University, Kafrelsheikh 33516, Egypt

<sup>3</sup>Department of Mathematics, Jamoum University College, Umm Al-Qura University, Makkah 21421, Saudi Arabia

(Received April 7, 2018, Revised May 23, 2018, Accepted May 28, 2018)

**Abstract.** Mechanical buckling of a rectangular functionally graded plate is obtained in the current paper using a refined higher-order shear and normal deformation theory. The impact of transverse normal strain is considered. The material properties are microscopically inhomogeneous and vary continuously based on a power law form in spatial direction. Navier's procedure is applied to examine the mechanical buckling behavior of a simply supported FG plate. The mechanical critical buckling subjected to uniaxial and biaxial compression loads are determined. The numerical investigation are compared with the numerical results in the literature. The influences of geometric parameters, power law index and different loading conditions on the critical buckling are studied.

**Keywords:** functionally graded plates; a refined higher-order normal and shear deformation theory; Navier's procedure; mechanical buckling analysis

## 1. Introduction

Functionally graded materials (FGMs) are advance composite materials were discovered by Japanese scientists in 1984. The material properties microscopically inhomogeneous and differ continuously in spatial direction which lead to uniform stress distribution. FGMs are a blend of metal and ceramic can be made in different order. The ceramic well known of its high-temperature resistance also play a major role in the prevention of oxidizing process of the metal whereas the metal helps stiffen the structure. FGMs help to solve some of the conventional materials problems such as matrix cracking, stress concentrations and interfacial debonding. There are diverse range of applications of FGM in astronautics, energy, biomedical and nuclear sectors.

The buckling analysis of FGM exposed to different loads conditions has been examined by many researchers such as Reddy (1997), Feldman and Aboudi (1997), Thai and Vo (2013), Yang *et al.* (2005), Neves *et al.* (2013), Fekrar (2012), Saha and Maiti (2012) and Mozafari and Ayob (2012). Huang and Li (2010) analyzed the mechanical buckling of FGM columns exposed to uniform compression and taking shear deformation into account and compared it with three columns theories. Kiani and Eslami (2010) examined the buckling temperature of FG columns in

---

\*Corresponding author, Professor, E-mail: [zenkour@kau.edu.sa](mailto:zenkour@kau.edu.sa)

accordance with the classical beam theory. Zenkour (2006) presented the governing equations of FGP employing a generalized shear deformation theory. Zhao *et al.* (2009) applied the element free kernel particle Ritz procedure to study the mechanical and buckling temperature of FGM plate.

The mechanical and buckling temperature of FG plates were numerically obtained according to three plate theories by Carrera (2005). Shen (2007) investigated the thermal post-buckling analysis with temperature-dependent properties of FGM plate. Matsunaga (2009) obtained thermal buckling and the critical thermal buckling using a 2D higher-order plate theory. Zenkour and Sobhy (2010) used three different thermal loads to examine the buckling temperature of FG plate. Bodaghi and Saidi (2011) analyzed the temperature stability of FG plate. Kiani and Eslami (2012) discussed the buckling temperature of imperfect FG plate with elastic foundation. The analytical solution of FGM hybrid composite plate exposed to mechanical fields was discussed by Birman (1995). Zenkour (2005) discussed the buckling of FG plate by employing higher-order plate theory. Lanhe (2004) presented the buckling temperature of FG plate. The analytical analysis of FG plate exposed to four thermal fields and the critical thermal buckling using Reddy's TSDT were presented by Javaheri and Eslami (2011). The first-order shear deformation theory is applied to investigate the buckling of FG plates by (Shariat and Eslami 2005, Yang *et al.* 2005, Zhao *et al.* 2009, Mokhtar *et al.* 2009, Sepiani *et al.* 2010 and Mohammadi *et al.* 2010).

The studies of the mechanical buckling using higher-order shear deformation theory which consider the normal effect are very limited. Therefore, in the current paper, a refined higher-order shear and normal deformation theory is applied to investigate the buckling behavior of a rectangular FG plate. The shear correction factor is neglected because the current theory takes into consideration the transverse impact. The equilibrium equations are determined using the principle of total potential energy. Navier's technique is applied to achieve a closed form solution of a simply supported FG plate. Numerical investigations are introduced to interpret the impact of geometric parameters and different loading conditions on the critical buckling and compared with the results in the literature.

## 2. Mathematical formulation

The current study examine a model of a simply supported rectangular functionally graded plate of dimensions length  $a$ , width  $b$  and thickness  $h$ . The plate is a blend of ceramic and metal where the upper surface is pure ceramic, the lower surface is pure metal, and the plate materials are graded continuously in  $z$  direction. The functionally graded material properties for instance modulus of elasticity  $E$  is supposed to differ across the plate thickness according to the power law form as

$$E(z) = E_m + (E_c - E_m) \left( \frac{1}{2} + \frac{z}{h} \right)^k, \quad (1)$$

where  $E_m$  and  $E_c$  are elasticity modulus of metal and ceramic material, respectively; and  $k$  is the power law or gradient index. Poisson's ratio  $\nu$  is fixed due to its small variation.

### 2.1 Displacement fields

The displacement field of the current shear and normal deformation theory can be expressed as (Zenkour 2007)

$$\begin{aligned}
 u_1(x, y, z) &= u - z \frac{\partial w}{\partial x} + \varphi(z)\theta_x, \\
 u_2(x, y, z) &= v - z \frac{\partial w}{\partial y} + \varphi(z)\theta_y, \\
 u_3(x, y, z) &= w + \eta \varphi'(z)\theta_z,
 \end{aligned}
 \tag{2}$$

where  $u$ ,  $v$  and  $w$  are in-plane displacements of the inner plane and  $u_1$ ,  $u_2$  and  $u_3$  are displacements in  $x$ ,  $y$  and  $z$  direction and  $\theta_x$ ,  $\theta_y$  and  $\theta_z$  represent the transverse normal rotations around the  $y$ ,  $x$  and  $z$  axes, respectively, and  $\varphi(z)$  is a shape function that used to obtain the non-classical higher-order plate theories. Note that  $\varphi'(z)$  is its first derivative with respect to  $z$ . Setting  $\varphi(z) = z \left[ \frac{1}{4} - \frac{5}{4} \left( \frac{z}{h} \right)^2 \right]$  gives the displacement of third-order shear deformation plate theory (TSDPT) by Reddy (1984). The impact of both transverse shear and normal strains are included, i.e.,  $\varepsilon_z \neq 0$  when  $\eta = 1$ , on the other hand, setting  $\eta = 0$  involves just the transverse shear deformation  $\varepsilon_z = 0$ . The strain-displacement relationships of Eq. (2) are given as

$$\begin{aligned}
 \begin{Bmatrix} \varepsilon_x \\ \varepsilon_y \\ \gamma_{xy} \end{Bmatrix} &= \begin{Bmatrix} \varepsilon_x^0 \\ \varepsilon_y^0 \\ \gamma_{xy}^0 \end{Bmatrix} + z \begin{Bmatrix} \varepsilon_x^1 \\ \varepsilon_y^1 \\ \gamma_{xy}^1 \end{Bmatrix} + \varphi(z) \begin{Bmatrix} \varepsilon_x^2 \\ \varepsilon_y^2 \\ \gamma_{xy}^2 \end{Bmatrix}, \\
 \begin{Bmatrix} \gamma_{yz} \\ \gamma_{xz} \end{Bmatrix} &= \varphi'(z) \begin{Bmatrix} \gamma_{yz}^0 \\ \gamma_{xz}^0 \end{Bmatrix}, \quad \varepsilon_z = \varphi''(z) \theta_z,
 \end{aligned}
 \tag{3}$$

where

$$\begin{Bmatrix} \varepsilon_x^0 \\ \varepsilon_y^0 \\ \gamma_{xy}^0 \end{Bmatrix} = \begin{Bmatrix} \frac{\partial u}{\partial x} \\ \frac{\partial v}{\partial y} \\ \frac{\partial u}{\partial y} + \frac{\partial v}{\partial x} \end{Bmatrix}, \quad \begin{Bmatrix} \varepsilon_x^1 \\ \varepsilon_y^1 \\ \gamma_{xy}^1 \end{Bmatrix} = - \begin{Bmatrix} \frac{\partial^2 w}{\partial x^2} \\ \frac{\partial^2 w}{\partial y^2} \\ 2 \frac{\partial^2 w}{\partial x \partial y} \end{Bmatrix},
 \tag{4a}$$

$$\begin{Bmatrix} \varepsilon_x^2 \\ \varepsilon_y^2 \\ \gamma_{xy}^2 \end{Bmatrix} = \begin{Bmatrix} \frac{\partial \theta_x}{\partial x} \\ \frac{\partial \theta_y}{\partial y} \\ \frac{\partial \theta_x}{\partial y} + \frac{\partial \theta_y}{\partial x} \end{Bmatrix}, \quad \begin{Bmatrix} \gamma_{yz}^0 \\ \gamma_{xz}^0 \end{Bmatrix} = \begin{Bmatrix} \theta_y + \frac{\partial \theta_z}{\partial y} \\ \theta_x + \frac{\partial \theta_z}{\partial x} \end{Bmatrix}.
 \tag{4b}$$

The constitutive equations of functionally graded materials when  $\varepsilon_z \neq 0$  can be written as

$$\begin{Bmatrix} \sigma_x \\ \sigma_y \\ \sigma_z \\ \tau_{yz} \\ \tau_{xz} \\ \tau_{xy} \end{Bmatrix} = \begin{bmatrix} c_{11} & c_{12} & c_{13} & 0 & 0 & 0 \\ c_{12} & c_{22} & c_{23} & 0 & 0 & 0 \\ c_{13} & c_{23} & c_{33} & 0 & 0 & 0 \\ 0 & 0 & 0 & c_{44} & 0 & 0 \\ 0 & 0 & 0 & 0 & c_{55} & 0 \\ 0 & 0 & 0 & 0 & 0 & c_{66} \end{bmatrix} \begin{Bmatrix} \varepsilon_x \\ \varepsilon_y \\ \varepsilon_z \\ \gamma_{yz} \\ \gamma_{xz} \\ \gamma_{xy} \end{Bmatrix},
 \tag{5}$$

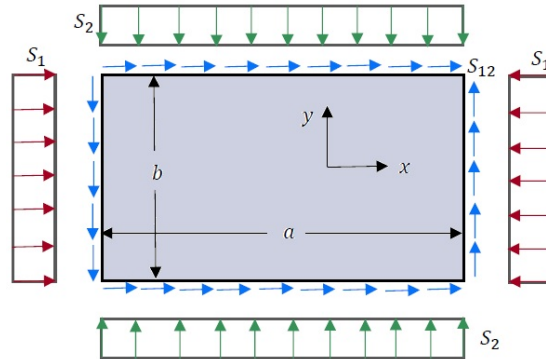


Fig. 1 Buckling of a FG rectangular plate under in-plane edge forces

where  $\sigma_i$ ,  $\varepsilon_i$ ,  $\tau_{ij}$  and  $\gamma_{ij}$  denote the normal stresses, normal strains, shear stresses and shear strains of the plate, respectively, ( $i, j = x, y$  and  $z$ ), and the three-dimensional elastic constants are written as

$$c_{11} = c_{22} = c_{33} = \frac{(1 - \nu) E(z)}{(1 + \nu)(1 - 2\nu)},$$

$$c_{12} = c_{13} = c_{23} = \frac{\nu E(z)}{(1 + \nu)(1 - 2\nu)}, \quad c_{44} = c_{55} = c_{66} = \frac{E(z)}{2(1 + \nu)}.$$

If  $\eta = 0$  ( $\varepsilon_z = 0$ ), then  $c_{ij}$  are given by

$$c_{11} = c_{22} = \frac{E(z)}{1 - \nu^2}, \quad c_{12} = \frac{\nu E(z)}{1 - \nu^2}, \quad c_{44} = c_{55} = c_{66} = \frac{E(z)}{2(1 + \nu)}.$$

The stress and moment resultants are demonstrated as

$$\{N_{ij}, M_{ij}, P_{ij}\} = \int_{-\frac{h}{2}}^{\frac{h}{2}} \sigma_{ij} \{1, z, \varphi(z)\} dz, \quad Q_z = \int_{-\frac{h}{2}}^{\frac{h}{2}} \sigma_z \varphi'(z) dz,$$

$$N_{zz} = \int_{-\frac{h}{2}}^{\frac{h}{2}} \sigma_z \varphi''(z) dz, \quad (i, j = x, y).$$

Substituting Eq. (5) in Eq. (8) then via integration across the thickness, we obtain

$$\begin{Bmatrix} N_x \\ N_y \\ M_x \\ M_y \\ P_x \\ P_y \\ Q_x \\ Q_y \end{Bmatrix} = \begin{bmatrix} A_{11} & A_{12} & B_{11} & B_{12} & B_{11}^* & B_{12}^* & G_{13}^* \\ A_{12} & A_{22} & B_{12} & B_{22} & B_{12}^* & B_{22}^* & G_{23}^* \\ B_{11} & B_{12} & D_{11} & D_{12} & D_{11}^* & D_{12}^* & H_{11}^* \\ B_{12} & B_{22} & D_{12} & D_{22} & D_{12}^* & D_{22}^* & H_{23}^* \\ B_{11}^* & B_{12}^* & D_{11}^* & D_{12}^* & F_{11}^* & F_{12}^* & L_{13}^* \\ B_{12}^* & B_{22}^* & D_{12}^* & D_{22}^* & F_{12}^* & F_{22}^* & L_{23}^* \\ G_{13}^* & G_{23}^* & H_{11}^* & H_{23}^* & L_{13}^* & L_{23}^* & J_{33}^* \end{bmatrix} \begin{Bmatrix} \varepsilon_x^0 \\ \varepsilon_y^0 \\ \varepsilon_x^1 \\ \varepsilon_y^1 \\ \varepsilon_x^2 \\ \varepsilon_y^2 \\ \varepsilon_z^0 \end{Bmatrix},$$

and

$$\begin{pmatrix} N_{xy} \\ M_{xy} \\ P_{xy} \end{pmatrix} = \begin{bmatrix} A_{66} & B_{66} & B_{66}^* \\ B_{66} & D_{66} & D_{66}^* \\ B_{66}^* & D_{66}^* & F_{66}^* \end{bmatrix} \begin{pmatrix} \gamma_{xy}^0 \\ \gamma_{xy}^1 \\ \gamma_{xy}^2 \end{pmatrix}, \quad \begin{pmatrix} Q_{yz} \\ Q_{xz} \end{pmatrix} \begin{bmatrix} J_{44}^* & 0 \\ 0 & J_{55}^* \end{bmatrix} \begin{pmatrix} \gamma_{yz}^0 \\ \gamma_{xz}^0 \end{pmatrix}, \quad (9b)$$

where the plate stiffness are expressed as

$$\begin{aligned} \{A_{ij}, B_{ij}, D_{ij}\} &= \int_{-\frac{h}{2}}^{\frac{h}{2}} c_{ij} \{1, z, z^2\} dz, \quad i, j = 1, 2, 6, \\ \{B_{ij}^*, D_{ij}^*, F_{ij}^*\} &= \int_{-\frac{h}{2}}^{\frac{h}{2}} c_{ij} \varphi(z) \{1, z, \varphi(z)\} dz, \\ \{G_{r3}^*, H_{r3}^*, L_{r3}^*\} &= \int_{-\frac{h}{2}}^{\frac{h}{2}} c_{r3} \varphi''(z) \{1, z, \varphi(z)\} dz, \quad r = 1, 2, \\ J_{\tau\tau}^* &= \int_{-\frac{h}{2}}^{\frac{h}{2}} c_{\tau\tau} (\varphi'(z))^2 dz, \quad \tau = 4, 5. \end{aligned} \quad (10)$$

### 3. Governing equations

The equilibrium equations can be determined by applying the principle of total potential energy as following

$$\delta(\Pi_1 + \Pi_2) = 0. \quad (11)$$

Here  $\Pi_1$  denotes strain energy and  $\Pi_2$  denotes work done by external forces. That is

$$\delta\Pi_1 + \delta\Pi_2 = \iiint_V (\sigma_i \delta\varepsilon_i + \tau_{ij} \delta\gamma_{ij}) dv + \int_A (\tilde{S} - q) \delta u_3 dA = 0, \quad (12)$$

where  $\tilde{S} = S_1 \frac{\partial^2 w}{\partial x^2} + 2S_{12} \frac{\partial^2 w}{\partial x \partial y} + S_2 \frac{\partial^2 w}{\partial y^2}$  and  $S_1$ ,  $S_2$  and  $S_{12}$  are the membrane forces caused by in-plane end loads and  $q$  is a transverse load as shown in Figure 1. The equations of equilibrium obtained by employing the integration by parts for Eq. (12) then setting the coefficients of  $\delta u$ ,  $\delta v$ ,  $\delta w$ ,  $\delta\theta_x$ ,  $\delta\theta_y$  and  $\delta\theta_z$  to zero, separately. Then, the equilibrium equations of the current theory are obtained as:

$$\begin{aligned}
\delta u: \frac{\partial N_x}{\partial x} + \frac{\partial N_{xy}}{\partial y} &= 0, & \delta v: \frac{\partial N_{xy}}{\partial x} + \frac{\partial N_y}{\partial y} &= 0, \\
\delta w: \frac{\partial^2 M_x}{\partial x^2} + 2 \frac{\partial^2 M_{xy}}{\partial x \partial y} + \frac{\partial^2 M_y}{\partial y^2} + \tilde{S} - q &= 0, & \delta \theta_x: \frac{\partial P_x}{\partial x} + \frac{\partial P_{xy}}{\partial y} - Q_{xz} &= 0, \\
\delta \theta_y: \frac{\partial P_{xy}}{\partial x} + \frac{\partial P_y}{\partial y} - Q_{yz} &= 0, & \delta \theta_z: \frac{\partial Q_{xz}}{\partial x} + \frac{\partial Q_{yz}}{\partial y} - N_z &= 0.
\end{aligned} \tag{13}$$

Substituting Eq. (9) into Eq. (13), the next form is constructed

$$[\zeta]\{A\} = \{0, 0, q, 0, 0, 0\}^t, \tag{14}$$

where  $\{A\} = \{u, v, w, \theta_x, \theta_y, \theta_z\}^t$  and the symmetric matrix  $[\zeta]$  is written as

$$\begin{aligned}
\zeta_{11} &= A_{11} \frac{\partial^2}{\partial x^2} + A_{66} \frac{\partial^2}{\partial y^2}, & \zeta_{12} &= (A_{12} + A_{66}) \frac{\partial^2}{\partial x \partial y}, & \zeta_{16} &= G_{13}^* \frac{\partial}{\partial x}, \\
\zeta_{13} &= -B_{11} \frac{\partial^3}{\partial x^3} - (B_{12} + 2B_{66}) \frac{\partial^3}{\partial x \partial y^2}, & \zeta_{14} &= B_{11}^* \frac{\partial^2}{\partial x^2} + B_{66}^* \frac{\partial^2}{\partial y^2}, \\
\zeta_{15} &= (B_{12}^* + B_{66}^*) \frac{\partial^2}{\partial x \partial y}, \\
\zeta_{22} &= A_{66} \frac{\partial^2}{\partial x^2} + A_{22} \frac{\partial^2}{\partial y^2}, & \zeta_{23} &= -B_{22} \frac{\partial^3}{\partial y^3} - (B_{12} + 2B_{66}) \frac{\partial^3}{\partial x^2 \partial y}, & \zeta_{26} &= G_{23}^* \frac{\partial}{\partial y}, \\
\zeta_{24} &= (B_{12}^* + B_{66}^*) \frac{\partial^2}{\partial x \partial y}, & \zeta_{25} &= B_{66}^* \frac{\partial^2}{\partial x^2} + B_{22}^* \frac{\partial^2}{\partial y^2}, & \zeta_{45} &= (F_{12}^* + F_{66}^*) \frac{\partial^2}{\partial x \partial y}, \\
\zeta_{33} &= D_{11} \frac{\partial^4}{\partial x^4} + 2(D_{12} + 2D_{66}) \frac{\partial^4}{\partial x^2 \partial y^2} + D_{22} \frac{\partial^4}{\partial y^4} + S_1 \frac{\partial^2}{\partial x^2} + S_2 \frac{\partial^2}{\partial y^2}, \\
\zeta_{46} &= (L_{13}^* - J_{55}^*) \frac{\partial}{\partial x}, & \zeta_{34} &= -D_{11}^* \frac{\partial^3}{\partial x^3} - (D_{12}^* + 2D_{66}^*) \frac{\partial^3}{\partial x^2 \partial y}, \\
\zeta_{35} &= -D_{22}^* \frac{\partial^3}{\partial y^3} - (D_{12}^* + 2D_{66}^*) \frac{\partial^3}{\partial x^2 \partial y}, \\
\zeta_{36} &= -H_{13}^* \frac{\partial^2}{\partial x^2} - H_{23}^* \frac{\partial^2}{\partial y^2}, & \zeta_{44} &= -J_{55}^* + F_{11}^* \frac{\partial^2}{\partial x^2} + F_{66}^* \frac{\partial^2}{\partial y^2}, & \zeta_{56} &= (L_{23}^* - J_{44}^*) \frac{\partial}{\partial y}, \\
\zeta_{55} &= -J_{44}^* + F_{66}^* \frac{\partial^2}{\partial x^2} + F_{22}^* \frac{\partial^2}{\partial y^2}, & \zeta_{66} &= J_{33}^* - J_{55}^* \frac{\partial^2}{\partial x^2} - J_{44}^* \frac{\partial^2}{\partial y^2}
\end{aligned} \tag{15}$$

#### 4. Exact solution of buckling of a rectangular FG plate

Navier's procedure is used to derive the exact solution of the mechanical buckling problem. The next boundary conditions are required at the side edges in order to apply this method

$$\begin{aligned} v = w = \theta_y = \theta_z = N_x = M_x = P_x = 0 & \quad \text{at } x = 0, a, \\ u = w = \theta_x = \theta_z = N_y = M_y = P_y = 0 & \quad \text{at } y = 0, b. \end{aligned} \tag{16}$$

To obtain the mechanical buckling loads, the transverse mechanical  $q$  and displacements expressions, which satisfy the boundary conditions, are chosen as

$$q = q_0 \sin(\lambda_m x) \sin(\mu_n y), \tag{17}$$

$$\begin{Bmatrix} u \\ v \\ w \\ \theta_x \\ \theta_y \\ \theta_z \end{Bmatrix} = \begin{Bmatrix} U \cos(\lambda_m x) \sin(\mu_n y) \\ V \sin(\lambda_m x) \cos(\mu_n y) \\ W \sin(\lambda_m x) \sin(\mu_n y) \\ X \cos(\lambda_m x) \sin(\mu_n y) \\ Y \sin(\lambda_m x) \cos(\mu_n y) \\ Z \sin(\lambda_m x) \sin(\mu_n y) \end{Bmatrix}, \tag{18}$$

where  $q_0$  is constant,  $\lambda_m = \frac{m\pi}{a}$ ,  $\mu_n = \frac{n\pi}{b}$ ,  $m$  and  $n$  are mode numbers,  $U, V, W, X, Y$  and  $Z$  are arbitrary parameters to be determined by substituting Eq. (18) into Eq. (15) and setting  $S_{12} = 0$ , then the following is obtained,

$$[\Gamma]\{\Lambda\} = \{0\}, \tag{19}$$

where  $\{\Lambda\} = \{U, V, W, X, Y, Z\}^t$ ,  $q_0 = 0$  and the symmetric matrix  $[\Gamma]$  is expressed as

$$\begin{aligned} \Gamma_{11} &= -\lambda_m^2 A_{11} - \mu_n^2 A_{66}, \quad \Gamma_{12} = -\lambda_m \mu_n (A_{12} + A_{66}), \quad \Gamma_{16} = \lambda_m G_{13}^*, \\ \Gamma_{13} &= \lambda_m^3 B_{11} + \lambda_m \mu_n^2 (B_{12} + 2B_{66}), \quad \Gamma_{14} = -\lambda_m^2 B_{11}^* - \mu_n^2 B_{66}^*, \quad \Gamma_{15} = -\lambda_m \mu_n (B_{12}^* + B_{66}^*), \\ \Gamma_{22} &= -\lambda_m^2 A_{66} - \mu_n^2 A_{22}, \quad \Gamma_{23} = \mu_n^3 B_{22} + \lambda_m^2 \mu_n (B_{12} + 2B_{66}), \quad \Gamma_{26} = \mu_n G_{23}^*, \\ \Gamma_{24} &= -\lambda_m \mu_n (B_{12}^* + B_{66}^*), \quad \Gamma_{25} = -\lambda_m^2 B_{66}^* - \mu_n^2 B_{22}^*, \quad \Gamma_{45} = -\lambda_m \mu_n (F_{12}^* + F_{66}^*), \\ \Gamma_{33} &= \lambda_m^4 D_{11} + 2\lambda_m^2 \mu_n^2 (D_{12} + 2D_{66}) + \mu_n^4 D_{22} - \lambda_m^2 S_1 - \mu_n^2 S_2, \\ \Gamma_{36} &= \lambda_m^2 H_{13}^* + \mu_n^2 H_{23}^*, \quad \Gamma_{34} = -\lambda_m^3 D_{11}^* - \lambda_m \mu_n^2 (D_{12}^* + 2D_{66}^*), \\ \Gamma_{35} &= -\mu_n^3 D_{22}^* - \lambda_m^2 \mu_n (D_{12}^* + 2D_{66}^*), \quad \Gamma_{44} = -J_{55}^* - \lambda_m^2 F_{11}^* - \mu_n^2 F_{66}^*, \\ \Gamma_{46} &= \lambda_m (L_{13}^* - J_{55}^*), \quad \Gamma_{55} = -J_{44}^* - \lambda_m^2 F_{66}^* - \mu_n^2 F_{22}^*, \\ \Gamma_{56} &= \mu_n (L_{23}^* - J_{44}^*), \quad \Gamma_{66} = J_{33}^* + \lambda_m^2 J_{55}^* + \mu_n^2 J_{44}^*. \end{aligned} \tag{20}$$

The nontrivial buckling loads can be derived by setting  $|\Gamma| = 0$ . The critical buckling load  $N_{cr}$  is the lower most buckling load for each  $m$  and  $n$  values.

### 5. Numerical results and discussions

A numerical analysis is performed to examine the mechanical buckling of a simply supported rectangular functionally graded pate subjected to different loads conditions. The plate is formed of

Table 1 The dimensionless critical buckling  $\tilde{N}_{cr}$  of an FG plate under uniaxial compression along the  $x$ -axis ( $a/b = 0.5$ ).

$a/h$	Source	$\varepsilon_z$	Gradient index ( $k$ )						
			0	0.5	1	2	5	10	20
5	Thai and Choi (2012)	=0	6.7203	4.4235	3.4164	2.6451	2.1484	1.9213	1.7115
	Reddy <i>et al.</i> (2013)	=0	6.714	4.409	3.39	2.61	2.124	1.90	1.705
	Present	=0	6.7203	4.4235	3.41635	2.6451	2.1484	1.9212	1.71152
	Present	$\neq 0$	6.963	4.630	3.618	2.830	2.283	2.018	1.782
10	Thai and Choi (2012)	=0	7.405	4.82	3.71	2.88	2.41	2.18	1.93
	Reddy <i>et al.</i> (2013)	=0	7.397	4.81	3.70	2.87	2.40	2.18	1.93
	Present	=0	7.4053	4.8206	3.7110	2.8896	2.4164	2.1895	1.9387
	Present	$\neq 0$	7.480	4.928	3.852	3.041	2.530	2.259	1.977
20	Thai and Choi (2012)	=0	7.599	4.93	3.79	2.95	2.49	2.26	2.00
	Reddy <i>et al.</i> (2013)	=0	7.590	4.924	3.78	2.95	2.48	2.26	2.00
	Present	=0	7.5992	4.9314	3.7930	2.9581	2.4944	2.2690	2.0054
	Present	$\neq 0$	7.619	5.007	3.914	3.098	2.599	2.328	2.032
50	Thai and Choi (2012)	=0	7.65	4.96	3.81	2.97	2.51	2.29	2.025
	Reddy <i>et al.</i> (2013)	=0	7.64	4.95	3.81	2.973	2.51	2.28	2.02
	Present	=0	7.6554	4.9634	3.8166	2.9779	2.5171	2.2922	2.0249
	Present	$\neq 0$	7.658	5.029	3.932	3.115	2.619	2.348	2.048
100	Thai and Choi (2012)	=0	7.66	4.968	3.82	2.98	2.52	2.29	2.028
	Reddy <i>et al.</i> (2013)	=0	7.65	4.96	3.81	2.97	2.51	2.292	2.02
	Present	=0	7.6635	4.9680	3.8200	2.9807	2.5204	2.2956	2.0277
	Present	$\neq 0$	7.664	5.033	3.934	3.117	2.622	2.351	2.050

Alumina ( $Al_2O_3$ ) as a ceramic and Aluminum ( $Al$ ) as metal. The plate material properties are graded through the  $z$  direction where the upper surface is pure ceramic ( $h/2$ ) while the lower surface is pure metal ( $-h/2$ ). The elasticity modulus of Alumina is  $E_c = 380$  GPa and Aluminum is  $E_m = 70$  GPa and Poisson's ratio is fixed across the plate's thickness  $\nu = 0.3$ . In this problem  $N_{cr} = \gamma_1 S_1$ ,  $S_2 = \gamma_2 S_1$ . The following dimensionless parameter is introduced

$$\tilde{N}_{cr} = \frac{N_{cr} a^2}{E_m h^3}. \quad (21)$$

### 5.1 Validation study

Here, a refined higher-order shear deformation theory considering  $\varepsilon_z \neq 0$  and  $\varepsilon_z = 0$  are used to analyze the mechanical buckling of simply-supported FG plates. Several numerical results are presented to confirm the accuracy of the current study. An investigation of the effects of aspect ratio, side-to-thickness ratio, gradient index and different loading conditions on the critical buckling of FG plates are carry out as following:

The dimensionless critical buckling of a simply-supported FG plate subjected to a uniaxial compression load ( $\gamma_1 = -1$ ,  $\gamma_2 = 0$ ), biaxial compression ( $\gamma_1 = \gamma_2 = -1$ ), and biaxial compression and tension ( $\gamma_1 = -1$ ,  $\gamma_2 = 1$ ), respectively are presented in Tables 1-12. The present results are compared with previous studies obtained using An efficient and simple refined theory (Quasi-3D) by Thai and Choi (2012), Higher-Order Shear Deformation Theory (HSDT) by Reddy *et al.* (2013) and an eight-unknown higher-order shear deformation theory (HSDT) by Thinh *et al.* (2016) for different values of gradient indexes  $k$ , side-to-thickness ratio  $a/h$  and aspect ratio  $a/b$ .

Table 2 The dimensionless critical buckling  $\tilde{N}_{cr}$  of an FG plate under uniaxial compression along the  $x$ -axis ( $a/b = 1$ )

$a/h$	Source	$\varepsilon_z$	Gradient index ( $k$ )						
			0	0.5	1	2	5	10	20
5	Thai and Choi (2012)	=0	16.02	10.62	8.22	6.34	5.05	4.48	4.00
	Reddy <i>et al.</i> (2013)	=0	16.00	10.57	8.146	6.23	4.97	4.44	3.98
	Present	=0	16.0210	10.6253	8.2244	6.3431	5.0530	4.4806	4.0069
	Present	≠0	16.866	11.288	8.823	6.855	5.418	4.755	4.225
10	Thai and Choi (2012)	=0	18.57	12.12	9.33	7.26	6.03	5.45	4.83
	Reddy <i>et al.</i> (2013)	=0	18.54	12.08	9.299	7.21	5.99	5.42	4.82
	Present	=0	18.5785	12.1229	9.3391	7.2630	6.0353	5.4528	4.8346
	Present	≠0	18.873	12.459	9.738	7.673	6.341	5.650	4.954
20	Thai and Choi (2012)	=0	19.35	12.56	9.66	7.53	6.34	5.76	5.09
	Reddy <i>et al.</i> (2013)	=0	19.31	12.53	9.649	7.51	6.32	5.75	5.08
	Present	=0	19.3527	12.5667	9.6674	7.5371	6.3447	5.7668	5.0988
	Present	≠0	18.873	12.778	9.989	7.903	6.618	5.925	5.173
50	Thai and Choi (2012)	=0	19.58	12.69	9.763	7.61	6.43	5.8	5.17
	Reddy <i>et al.</i> (2013)	=0	19.54	12.67	9.743	7.601	6.42	5.84	5.16
	Present	=0	19.5814	12.6970	9.7636	7.6176	6.4372	5.8613	5.1781
	Present	≠0	19.594	12.870	10.061	7.969	6.700	6.006	5.238
100	Thai and Choi (2012)	=0	19.61	12.71	9.77	7.62	6.45	5.87	5.18
	Reddy <i>et al.</i> (2013)	=0	19.57	12.69	9.75	7.61	6.43	5.86	5.17
	Present	=0	19.6145	12.7158	9.7775	7.6293	6.4507	5.87515	5.1896
	Present	≠0	19.617	12.883	10.071	7.979	6.712	6.018	5.247

Table 3 The dimensionless critical buckling  $\tilde{N}_{cr}$  of an FG plate under uniaxial compression along the  $x$ -axis ( $a/b = 1.5$ )

$a/h$	Source	$\varepsilon_z$	Gradient index ( $k$ ) <sup>a</sup>						
			0	0.5	1	2	5	10	20
5	Thai and Choi (2012)	=0	28.19	19.25	15.03	11.4234	8.47	7.29	6.61
	Reddy <i>et al.</i> (2013)	=0	28.15	19.09	14.76	11.06	8.25	7.20	6.56
	Present	=0	28.1995	19.2510	15.0343	11.4233	8.4727	7.2952	6.6105
	Present	≠0	30.950	21.279	16.673	12.648	9.253	7.913	7.175
10	Thai and Choi (2012)	=0	40.74	26.90	20.80	16.07	12.95	11.53	10.29
	Reddy <i>et al.</i> (2013)	=0	40.58	26.72	20.57	15.81	12.74	11.42	10.22
	Present	=0	40.7475	26.9091	20.8024	16.0792	12.9500	11.537	10.2957
	Present	≠0	42.521	28.351	22.160	17.281	13.820	12.175	10.783
20	Thai and Choi (2012)	=0	45.89	29.90	23.02	17.92	14.94	13.52	11.98
	Reddy <i>et al.</i> (2013)	=0	45.64	29.71	22.85	17.75	14.81	13.425	11.90
	Present	=0	45.8930	29.9049	23.0285	17.9221	14.9471	13.5273	11.9843
	Present	≠0	46.470	30.642	23.951	18.893	15.673	13.983	12.247
50	Thai and Choi (2012)	=0	47.57	30.86	23.74	18.51	15.628	14.21	12.56
	Reddy <i>et al.</i> (2013)	=0	47.29	30.67	23.59	18.39	15.51	14.12	12.48
	Present	=0	47.5786	30.8690	23.7414	18.5177	15.6237	14.2156	12.5628
	Present	≠0	47.678	31.330	24.492	19.391	16.277	14.583	12.725
100	Thai and Choi (2012)	=0	47.82	31.01	23.84	18.60	15.72	14.31	12.65
	Reddy <i>et al.</i> (2013)	=0	47.53	30.82	23.69	18.48	15.62	14.23	12.57
	Present	=0	47.8297	31.0119	23.8469	18.6061	15.7255	14.3198	12.6501
	Present	≠0	47.854	31.430	24.570	19.463	16.367	14.672	12.796

<sup>a</sup>Mode number ( $m, n$ ) = (2, 1)

Table 4 The dimensionless critical buckling  $\tilde{N}_{cr}$  of an FG plate under uniaxial compression along the  $x$ -axis ( $a/b = 2$ )

$a/h$	Source	$\varepsilon_z$	Gradient index ( $k$ )						
			0	0.5	1	2	5	10	20
5	Thai and Choi (2012)	=0	37.74 <sup>b</sup>	26.36 <sup>b</sup>	20.74 <sup>b</sup>	15.58 <sup>b</sup>	10.95 <sup>b</sup>	9.15 <sup>c</sup>	8.39 <sup>c</sup>
	Reddy <i>et al.</i> (2013)	=0	37.67 <sup>b</sup>	26.11 <sup>b</sup>	20.29 <sup>b</sup>	14.99 <sup>b</sup>	10.65 <sup>b</sup>	9.04 <sup>c</sup>	8.317 <sup>c</sup>
	Present	=0	37.7403 <sup>b</sup>	26.3644 <sup>b</sup>	20.7490 <sup>b</sup>	15.5819 <sup>b</sup>	10.9554 <sup>b</sup>	9.1505 <sup>c</sup>	8.3987 <sup>c</sup>
	Present	≠0	40.812 <sup>b</sup>	28.675 <sup>b</sup>	22.627 <sup>b</sup>	16.955 <sup>b</sup>	11.767 <sup>b</sup>	9.458 <sup>c</sup>	8.672 <sup>c</sup>
10 <sup>a</sup>	Thai and Choi (2012)	=0	64.08	42.50	32.89	25.37	20.21	17.92	16.02
	Reddy <i>et al.</i> (2013)	=0	63.78	42.14	32.46	24.86	19.84	17.72	15.90
	Present	=0	64.0842	42.5015	32.8979	25.3726	20.2122	17.9227	16.0279
	Present	≠0	67.466	45.152	35.294	27.421	21.674	19.020	16.902
20 <sup>a</sup>	Thai and Choi (2012)	=0	74.3	48.49	37.35	29.05	24.14	21.81	19.33
	Reddy <i>et al.</i> (2013)	=0	73.80	48.10	37.00	28.71	23.86	21.61	19.18
	Present	=0	74.3140	48.4917	37.3564	29.0522	24.1412	21.811	19.3385
	Present	≠0	75.495	49.836	38.954	30.692	25.364	22.600	19.817
50 <sup>a</sup>	Thai and Choi (2012)	=0	77.80	50.48	38.83	30.28	25.53	23.227	20.53
	Reddy <i>et al.</i> (2013)	=0	77.20	50.09	38.51	30.02	25.32	23.04	20.36
	Present	=0	77.8003	50.4890	38.8337	30.2857	25.5363	23.2278	20.5301
	Present	≠0	78.008	51.270	40.079	31.726	26.614	23.838	20.805
100 <sup>a</sup>	Thai and Choi (2012)	=0	78.32	50.78	39.05	30.47	25.74	23.45	20.71
	Reddy <i>et al.</i> (2013)	=0	77.71	50.38	38.74	30.22	25.54	23.26	20.55
	Present	=0	78.3256	50.7880	39.0545	30.4707	25.7491	23.4455	20.7126
	Present	≠0	78.378	51.480	40.244	31.878	26.802	24.026	20.954

<sup>a</sup>Mode number  $(m, n) = (2, 1)$ , <sup>b</sup>Mode number  $(m, n) = (3, 1)$ , <sup>c</sup>Mode number  $(m, n) = (4, 1)$

Table 5 The dimensionless critical buckling  $\tilde{N}_{cr}$  of an FG plate under biaxial compression ( $a/b = 0.5$ )

$a/h$	Source	$\varepsilon_z$	Gradient index ( $k$ )						
			0	0.5	1	2	5	10	20
5	Thai and Choi (2012)	=0	5.376	3.539	2.733	2.116	1.719	1.537	1.369
	Reddy <i>et al.</i> (2013)	=0	5.371	3.527	2.715	2.092	1.700	1.527	1.364
	Thinh <i>et al.</i> (2016)	≠0	5.4090	3.5652	2.7563	2.1348	1.7320	1.5474	1.3772
	Present	=0	5.3762	3.5388	2.7330	2.1160	1.7187	1.5370	1.3692
10	Present	≠0	5.570	3.704	2.895	2.264	1.826	1.614	1.426
	Thai and Choi (2012)	=0	5.926	3.857	2.969	2.312	1.933	1.752	1.551
	Reddy <i>et al.</i> (2013)	=0	5.918	3.850	2.961	2.302	1.925	1.747	1.548
	Thinh <i>et al.</i> (2016)	≠0	5.9343	3.8644	2.9758	2.3174	1.9374	1.7551	1.5536
20	Present	=0	5.9242	3.8565	2.9688	2.3117	1.9331	1.7516	1.5509
	Present	≠0	5.984	3.942	3.082	2.433	2.024	1.807	1.581
	Thai and Choi (2012)	=0	6.079	3.9451	3.034	2.367	1.996	1.815	1.604
	Reddy <i>et al.</i> (2013)	=0	6.072	3.940	3.029	2.362	1.991	1.812	1.602
50	Thinh <i>et al.</i> (2016)	≠0	6.0821	3.9473	3.0363	2.3680	1.9967	1.8161	1.6051
	Present	=0	6.0794	3.9451	3.0344	2.3665	1.9955	1.8152	1.6043
	Present	≠0	6.095	4.006	3.131	2.478	2.079	1.862	1.625
	Thai and Choi (2012)	=0	6.124	3.971	3.053	2.382	2.014	1.834	1.620
100	Reddy <i>et al.</i> (2013)	=0	6.117	3.966	3.049	2.379	2.011	1.831	1.618
	Thinh <i>et al.</i> (2016)	≠0	6.1248	3.9711	3.0536	2.3826	2.0139	1.8340	1.6201
	Present	=0	6.1243	3.9707	3.0533	2.3823	2.0137	1.8338	1.6199
	Present	≠0	6.126	4.023	3.145	2.492	2.095	1.878	1.638
100	Thai and Choi (2012)	=0	6.131	3.974	3.056	2.385	2.016	1.837	1.622
	Reddy <i>et al.</i> (2013)	=0	6.123	3.970	3.052	2.382	2.014	1.834	1.620
	Thinh <i>et al.</i> (2016)	≠0	6.1309	3.9745	3.0561	2.3847	2.0164	1.8366	1.6223
	Present	=0	6.1308	3.9744	3.0560	2.3846	2.0163	1.8365	1.6222
Present	≠0	6.131	4.026	3.147	2.493	2.098	1.881	1.640	

Table 6 The dimensionless critical buckling  $\tilde{N}_{cr}$  of an FG plate under biaxial compression ( $a/b = 1$ )

$a/h$	Source	$\varepsilon_z$	Gradient index ( $k$ )						
			0	0.5	1	2	5	10	20
5	Thai and Choi (2012)	=0	8.011	5.313	4.112	3.172	2.527	2.240	2.004
	Reddy <i>et al.</i> (2013)	=0	8.001	5.288	4.073	3.120	2.487	2.221	1.994
	Thinh <i>et al.</i> (2016)	≠0	8.0826	5.3716	4.1643	3.2132	2.5549	2.2621	2.0205
	Present	=0	8.0105	5.3126	4.1122	3.1715	2.5265	2.2403	2.0034
	Present	≠0	8.433	5.644	4.411	3.427	2.709	2.377	2.112
10	Thai and Choi (2012)	=0	9.289	6.062	4.670	3.632	3.018	2.726	2.417
	Reddy <i>et al.</i> (2013)	=0	9.273	6.045	4.650	3.608	2.998	2.715	2.410
	Thinh <i>et al.</i> (2016)	≠0	9.3139	6.0810	4.6867	3.6455	3.0280	2.7346	2.4236
	Present	=0	9.2892	6.0614	4.6695	3.6315	3.0176	2.7264	2.4173
	Present	≠0	9.436	6.229	4.869	3.836	3.170	2.825	2.477
20	Thai and Choi (2012)	=0	9.676	6.283	4.834	3.769	3.172	2.883	2.549
	Reddy <i>et al.</i> (2013)	=0	9.658	6.270	4.821	3.757	3.162	2.876	2.544
	Thinh <i>et al.</i> (2016)	≠0	9.6831	6.2887	4.8384	3.7723	3.1753	2.8857	2.5512
	Present	=0	9.6763	6.2833	4.8337	3.7685	3.1723	2.8834	2.5494
	Present	≠0	9.716	6.389	4.994	3.951	3.309	2.962	2.586
50	Thai and Choi (2012)	=0	9.791	6.349	4.882	3.809	3.219	2.931	2.589
	Reddy <i>et al.</i> (2013)	=0	9.772	6.336	4.872	3.801	3.212	2.925	2.584
	Thinh <i>et al.</i> (2016)	≠0	9.7918	6.3494	4.8826	3.8095	3.2191	2.9311	2.5894
	Present	=0	9.7907	6.3485	4.8818	3.8088	3.2186	2.9306	2.5890
	Present	≠0	9.797	6.435	5.030	3.984	3.350	3.003	2.619
100	Thai and Choi (2012)	=0	9.807	6.358	4.889	3.815	3.225	2.938	2.595
	Reddy <i>et al.</i> (2013)	=0	9.788	6.345	4.879	3.807	3.219	2.932	2.590
	Thinh <i>et al.</i> (2016)	≠0	9.8075	6.3581	4.8890	3.8148	3.2255	2.9377	2.5949
	Present	=0	9.8072	6.3579	4.8887	3.8146	3.2253	2.9375	2.5948
	Present	≠0	9.808	6.441	5.035	3.989	3.356	3.009	2.623

Table 7 The dimensionless critical buckling  $\tilde{N}_{cr}$  of an FG plate under biaxial compression ( $a/b = 1.5$ )

$a/h$	Source	$\varepsilon_z$	Gradient index ( $k$ )						
			0	0.5	1	2	5	10	20
5	Thai and Choi (2012)	=0	11.682	7.830	6.080	4.664	3.618	3.172	2.851
	Reddy <i>et al.</i> (2013)	=0	11.665	7.782	6.000	4.559	3.544	3.138	2.833
	Present	=0	11.6819	7.8298	6.0799	4.6636	3.6175	3.1718	2.8510
	Present	≠0	12.540	8.473	6.626	5.101	3.91	3.405	3.050
	Thai and Choi (2012)	=0	14.608	9.569	7.379	5.728	4.712	4.238	3.766
10	Reddy <i>et al.</i> (2013)	=0	14.571	9.528	7.331	5.671	4.666	4.212	3.749
	Present	=0	14.6084	9.5685	7.3793	5.7278	4.7124	4.2384	3.7657
	Present	≠0	14.971	9.913	7.74	6.085	4.977	4.418	3.887
	Thai and Choi (2012)	=0	15.589	10.133	7.798	6.076	5.101	4.630	4.096
	Reddy <i>et al.</i> (2013)	=0	15.542	10.098	7.766	6.046	5.075	4.611	4.082
20	Present	=0	15.5887	10.1331	7.7976	6.0761	5.1006	4.6299	4.0961
	Present	≠0	15.693	10.327	8.073	6.381	5.329	4.765	4.165
	Thai and Choi (2012)	=0	15.888	10.3036	7.924	6.182	5.221	4.753	4.200
	Reddy <i>et al.</i> (2013)	=0	15.837	10.270	7.897	6.160	5.203	4.737	4.186
	Present	=0	15.8875	10.3036	7.9235	6.1815	5.2212	4.7530	4.1994
50	Present	≠0	15.904	10.448	8.167	6.468	5.436	4.872	4.249
	Thai and Choi (2012)	=0	15.931	10.328	7.942	6.197	5.239	4.771	4.215
	Reddy <i>et al.</i> (2013)	=0	15.880	10.295	7.916	6.177	5.222	4.756	4.201
	Present	=0	15.9311	10.3284	7.9419	6.1968	5.2389	4.7712	4.2146
	Present	≠0	15.935	10.465	8.181	6.481	5.451	4.887	4.262

Table 8 The dimensionless critical buckling  $\tilde{N}_{\sigma}$  of an FG plate under biaxial compression ( $a/b = 2$ )

$a/h$	Source	$\varepsilon_z$	Gradient index ( $k$ )						
			0	0.5	1	2	5	10	20
5	Thai and Choi (2012)	=0	15.724	10.662	8.309	6.335	4.775	4.138	3.739
	Reddy <i>et al.</i> (2013)	=0	15.698	10.581	8.172	6.156	4.661	4.088	3.712
	Present	=0	15.7234	10.6622	8.3091	6.3353	4.7753	4.1382	3.7392
	Present	≠0	17.156	11.719	9.174	6.995	5.207	4.479	4.044
10	Thai and Choi (2012)	=0	21.505	14.155	10.932	8.464	6.875	6.148	5.477
	Reddy <i>et al.</i> (2013)	=0	21.429	14.071	10.830	8.345	6.782	6.095	5.444
	Present	=0	21.5049	14.1552	10.9323	8.4643	6.8749	6.1481	5.4768
	Present	≠0	22.283	14.816	11.580	9.056	7.307	6.458	5.704
20	Thai and Choi (2012)	=0	23.697	15.426	11.875	9.247	7.737	7.007	6.204
	Reddy <i>et al.</i> (2013)	=0	23.590	15.346	11.802	9.177	7.674	6.964	6.171
	Present	=0	23.6970	15.4260	11.8755	9.2469	7.7326	7.0067	6.2039
	Present	≠0	23.938	15.771	12.328	9.733	8.096	7.230	6.327
50	Thai and Choi (2012)	=0	24.394	15.824	12.170	9.493	8.013	7.293	6.444
	Reddy <i>et al.</i> (2013)	=0	24.276	15.746	12.108	9.442	7.970	7.255	6.412
	Present	=0	24.3944	15.8243	12.1699	9.4931	8.0132	7.2925	6.4440
	Present	≠0	24.435	16.054	12.550	9.938	8.346	7.478	6.524
100	Thai and Choi (2012)	=0	24.497	15.883	12.213	9.529	8.055	7.335	6.480
	Reddy <i>et al.</i> (2013)	=0	24.378	15.805	12.153	9.482	8.015	7.299	6.448
	Present	=0	24.4974	15.8830	12.2132	9.5293	8.0549	7.3353	6.4798
	Present	≠0	24.507	16.095	12.582	9.968	8.383	7.515	6.554

Table 9 The dimensionless critical buckling  $\tilde{N}_{\sigma}$  of an FG plate under biaxial compression and tension ( $a/b = 0.5$ )

$a/h$	Source	$\varepsilon_z$	Gradient index ( $k$ )						
			0	0.5	1	2	5	10	20
5	Thai and Choi (2012)	=0	8.960	5.898	4.555	3.527	2.865	2.562	2.282
	Reddy <i>et al.</i> (2013)	=0	8.953	5.879	4.525	3.487	2.833	2.545	2.274
	Present	=0	8.9604	5.8980	4.5551	3.5268	2.8645	2.5617	2.2820
	Present	≠0	9.2847	6.17352	4.8251	3.7734	3.0449	2.6908	2.3768
10	Thai and Choi (2012)	=0	9.874	6.428	4.948	3.853	3.222	2.919	2.585
	Reddy <i>et al.</i> (2013)	=0	9.863	6.416	4.934	3.837	3.208	2.911	2.580
	Present	=0	9.8737	6.4275	4.9481	3.8528	3.2219	2.9194	2.5849
	Present	≠0	9.9741	6.5715	5.1368	4.0555	3.3735	3.0127	2.6364
20	Thai and Choi (2012)	=0	10.132	6.575	5.057	3.944	3.326	3.025	2.674
	Reddy <i>et al.</i> (2013)	=0	10.120	6.566	5.049	3.936	3.319	3.020	2.670
	Present	=0	10.1323	6.5752	5.05737	3.9442	3.3259	3.0253	2.6739
	Present	≠0	10.1589	6.6767	5.2193	4.1316	3.4662	3.1047	2.7096
50	Thai and Choi (2012)	=0	10.207	6.618	5.089	3.971	3.356	3.056	2.700
	Reddy <i>et al.</i> (2013)	=0	10.195	6.610	5.082	3.965	3.352	3.052	2.697
	Present	=0	10.2072	6.6179	5.0888	3.9705	3.3562	3.0563	2.6999
	Present	≠0	10.2115	6.7066	5.2428	4.1533	3.4930	3.1315	2.7308
100	Thai and Choi (2012)	=0	10.218	6.624	5.093	3.974	3.361	3.061	2.704
	Reddy <i>et al.</i> (2013)	=0	10.206	6.616	5.087	3.969	3.356	3.057	2.700
	Present	=0	10.2180	6.6240	5.0933	3.9743	3.3606	3.0608	2.7037
	Present	≠0	10.2191	6.7109	5.2462	4.1564	3.4968	3.1353	2.7338

Table 10 The dimensionless critical buckling  $\tilde{N}_{cr}$  of an FG plate under biaxial compression and tension ( $a/b = 1$ )

$a/h$	Source	$\varepsilon_z$	Gradient index ( $k$ )						
			0	0.5	1	2	5	10	20
5 <sup>a</sup>	Thai and Choi (2012)	=0	26.20	17.77	13.84	10.55	7.95	6.89	6.23
	Reddy <i>et al.</i> (2013)	=0	26.16	17.63	13.62	10.26	7.76	6.81	6.18
	Present	=0	26.2057	17.7703	13.8486	10.5589	7.9589	6.8970	6.2320
	Present	≠0	28.5947	19.5332	15.2906	11.6593	8.6794	7.4659	6.7411
10 <sup>a</sup>	Thai and Choi (2012)	=0	35.84	23.59 <sup>b</sup>	18.22	14.10	11.45	10.24	9.12
	Reddy <i>et al.</i> (2013)	=0	35.71	23.45 <sup>b</sup>	18.04	13.90	11.30	10.15	9.07
	Present	=0	35.8416	23.5920 <sup>b</sup>	18.2205	14.1072	11.4582	10.2468	9.1281
	Present	≠0	37.1388	24.6940 <sup>b</sup>	19.3007	15.0937	12.1798	10.7635	9.5072
20 <sup>a</sup>	Thai and Choi (2012)	=0	39.49	25.71	19.79	15.41	12.88	11.67	10.34
	Reddy <i>et al.</i> (2013)	=0	39.31	25.57	19.67	15.29	12.79	11.60	10.28
	Present	=0	39.4950	25.710	19.7925	15.4115	12.8877	11.6778	10.3399
	Present	≠0	39.8966	26.2863	20.5473	16.2221	13.4941	12.0509	10.5458
50 <sup>a</sup>	Thai and Choi (2012)	=0	40.65	26.37	20.283	15.82	13.35	12.15	10.74 <sup>b</sup>
	Reddy <i>et al.</i> (2013)	=0	40.46	26.24	20.179	15.73	13.28	12.09	10.68 <sup>b</sup>
	Present	=0	40.6573	26.3739	20.2832	15.8218	13.3553	12.1542	10.7400 <sup>b</sup>
	Present	≠0	40.7257	26.7581	20.9177	16.5635	13.9106	12.4647	10.8748 <sup>b</sup>
100 <sup>a</sup>	Thai and Choi (2012)	=0	40.82	26.47	20.35	15.88	13.42	12.22	10.79 <sup>b</sup>
	Reddy <i>et al.</i> (2013)	=0	40.62	26.34	20.25	15.80	13.35	12.16	10.74 <sup>b</sup>
	Present	=0	40.8290	26.4716	20.3553	15.8822	13.4249	12.2255	10.7998 <sup>b</sup>
	Present	≠0	40.8463	26.8265	20.9714	16.6133	13.9720	12.5260	10.9233 <sup>b</sup>

<sup>a</sup>Mode number  $(m, n) = (2, 1)$ , <sup>b</sup>Mode number  $(m, n) = (1, 2)$

Table 11 The dimensionless critical buckling  $\tilde{N}_{cr}$  of an FG plate under biaxial compression and tension ( $a/b = 1.5$ )

$a/h$	Source	$\varepsilon_z$	Gradient index ( $k$ )						
			0	0.5	1	2	5	10	20
5 <sup>a</sup>	Thai and Choi (2012)	=0	29.02	20.11	15.78	11.90	8.52	7.24	6.60
	Reddy <i>et al.</i> (2013)	=0	28.97	19.92	15.45	11.47	8.29	7.15	6.54
	Present	=0	29.0249	20.1104	15.7822	11.9008	8.5249	7.2421	6.6007
	Present	≠0	31.8161	22.1880	17.4498	13.1142	9.2575	7.8206	7.1434
10	Thai and Choi (2012)	=0	37.982	24.878	19.186	14.893	12.252	11.020	9.791
	Reddy <i>et al.</i> (2013)	=0	37.884	24.773	19.060	14.745	12.133	10.950	9.748
	Present	=0	37.9819	24.8781	19.1862	14.8924	12.2522	11.0198	9.7909
	Present	≠0	38.9253	25.7755	20.1463	15.8219	12.9408	11.4891	10.1069
20	Thai and Choi (2012)	=0	40.531	26.346	20.274	15.798	13.262	12.038	10.650
	Reddy <i>et al.</i> (2013)	=0	40.408	26.255	20.190	15.718	13.194	11.988	10.612
	Present	=0	40.5306	26.3462	20.2739	15.7979	13.2615	12.0378	10.6499
	Present	≠0	40.8022	26.8522	20.9903	16.5920	13.856	12.3912	10.8301
50	Thai and Choi (2012)	=0	41.308	26.789	20.601	16.072	13.575	12.358	10.919
	Reddy <i>et al.</i> (2013)	=0	41.177	26.702	20.532	16.016	13.528	12.317	10.883
	Present	=0	41.3076	26.7893	20.6013	16.0719	13.5751	12.3580	10.9186
	Present	≠0	41.3528	27.1650	21.2359	16.8189	14.1343	12.6682	11.0499
100	Thai and Choi (2012)	=0	41.421	26.854	20.649	16.112	13.621	12.405	10.958
	Reddy <i>et al.</i> (2013)	=0	41.289	26.768	20.582	16.059	13.577	12.365	10.923
	Present	=0	41.4210	26.8539	20.6489	16.1118	13.6212	12.4051	10.9581
	Present	≠0	41.4324	27.2101	21.2714	16.8518	14.1749	12.7087	11.0820

<sup>a</sup>Mode number  $(m, n) = (1, 2)$

Table 12 The dimensionless critical buckling  $\tilde{N}_{cr}$  of a simply-supported FG plate under biaxial compression and tension ( $a/b = 2$ )

$a/h$	Source	$\varepsilon_z$	Gradient index ( $k$ )						
			0	0.5	1	2	5	10	20
5	Thai and Choi (2012)	=0	26.206	17.770	13.849	10.559	7.959	6.897	6.232
	Reddy <i>et al.</i> (2013)	=0	26.164	17.636	13.620	10.261	7.768	6.814	6.187
	Present	=0	26.2057	17.7703	13.8486	10.5589	7.9589	6.8970	6.2320
	Present	$\neq 0$	28.5947	19.5332	15.2906	11.6593	8.67940	7.4659	6.7411
10	Thai and Choi (2012)	=0	35.842	23.592	18.221	14.107	11.458	10.247	9.128
	Reddy <i>et al.</i> (2013)	=0	35.715	23.451	18.050	13.909	11.303	10.159	9.073
	Present	=0	35.8416	23.5920	18.2205	14.1072	11.4582	10.2468	9.1281
	Present	$\neq 0$	37.1388	24.6940	19.3007	15.0937	12.1798	10.7635	9.5072
20	Thai and Choi (2012)	=0	39.495	25.710	19.793	15.412	12.888	11.678	10.340
	Reddy <i>et al.</i> (2013)	=0	39.317	25.576	19.670	15.295	12.791	11.607	10.286
	Present	=0	39.4950	25.7100	19.7925	15.4115	12.8877	11.6778	10.3399
	Present	$\neq 0$	39.8966	26.2863	20.5473	16.2221	13.4941	12.0509	10.5458
50	Thai and Choi (2012)	=0	40.657	26.374	20.283	15.822	13.355	12.154	10.740
	Reddy <i>et al.</i> (2013)	=0	40.460	26.243	20.179	15.737	13.284	12.092	10.687
	Present	=0	40.6573	26.3739	20.2832	15.8218	13.3553	12.1542	10.7400
	Present	$\neq 0$	40.7257	26.7581	20.9177	16.5635	13.9106	12.4647	10.8748
100	Thai and Choi (2012)	=0	40.829	26.472	20.355	15.882	13.425	12.226	10.800
	Reddy <i>et al.</i> (2013)	=0	40.629	26.341	20.254	15.803	13.358	12.165	10.747
	Present	=0	40.8290	26.4716	20.3553	15.8822	13.4249	12.2255	10.7998
	Present	$\neq 0$	40.8463	26.8265	20.9714	16.6133	13.9720	12.5260	10.9233

It can be observed from these tables that the critical buckling decreases as the gradient index increases and the fully ceramic has the greatest critical buckling of all. This is predictable because ceramic has lower strength than metal. In addition, the increase of thickness ratio and aspect ratio lead to increasing in the critical buckling also it may change the buckling modes. Moreover, It is apparent that the critical buckling under uniaxial compression in Tables 1-4 had higher values than both of the critical buckling under biaxial compression in Tables 5-8 and compression and tension in Tables 9-12.

It can be found that the results of the current shear deformation theory with  $\varepsilon_z = 0$  are in excellent agreement with those by Thai and Choi (2012) and Reddy *et al.* (2013) while the present results with  $\varepsilon_z \neq 0$  slightly differ when the plate is thick and agreed well when the plate gets thinner as the researchers considered  $\varepsilon_z = 0$ . This comparison addresses the strong influence of the inclusion of normal strain on the critical buckling of FG plates especially thicker ones. As it observed from the above tables that the critical buckling with  $\varepsilon_z \neq 0$  is higher than  $\varepsilon_z = 0$  when aspect ratio is increasing and both of gradient index and thickness ratio decreasing. This show that the normal strain can be affected by the FG material, plate structure and on the involved geometric parameters. Furthermore, the present results agreed with the corresponding results of Thinh *et al.* (2016) where  $\varepsilon_z \neq 0$  is considered.

### 5.2 Parametric study

The influence of geometric parameters  $a/h$  and  $a/b$  on dimensionless critical buckling load of a simply-supported rectangular FG plate are presented with several loading conditions and various gradient index  $k$  values in Figures 2-5. The FG plate is formed of  $Al/Al_2O_3$ .

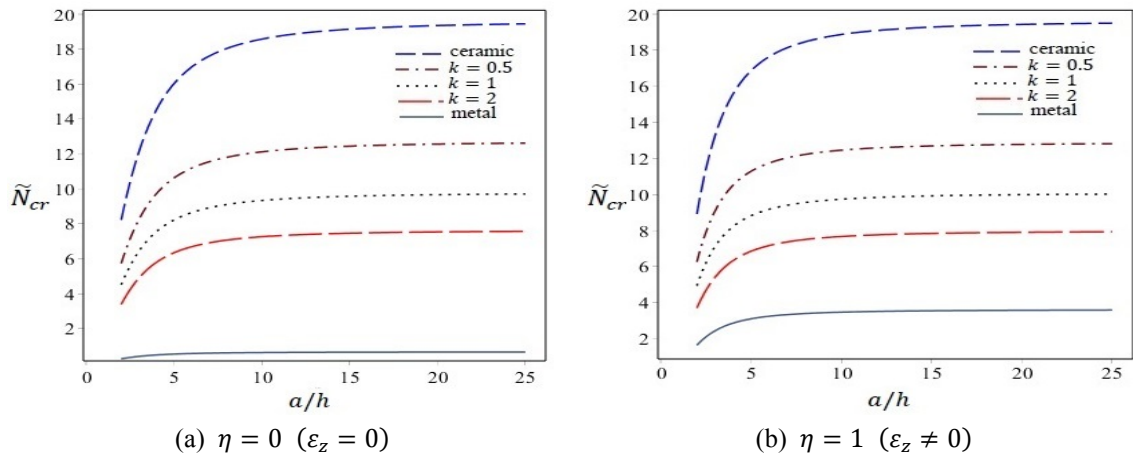


Fig. 2 The influence of side-to-thickness ratios ( $a/h$ ) on dimensionless critical buckling ( $\tilde{N}_{cr}$ ) of an FG plate under uniaxial compression for several gradient index ( $k$ ) when  $a/b = 1$

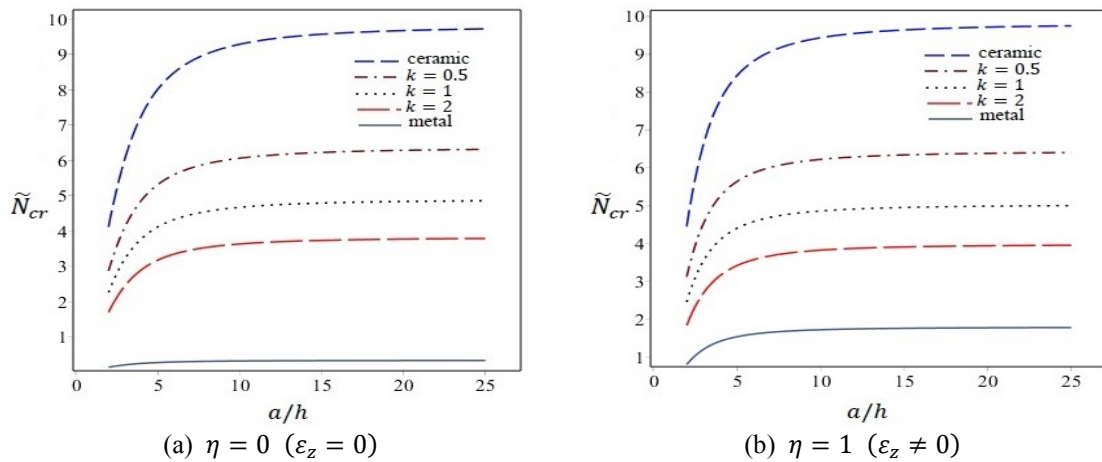


Fig. 3 The influence of side-to-thickness ratios ( $a/h$ ) on dimensionless critical buckling ( $\tilde{N}_{cr}$ ) of an FG plate under biaxial compression for several gradient index ( $k$ ) when  $a/b = 1$

Figures 2 and 3 illustrate the dimensionless critical buckling under uniaxial and biaxial compression versus side-to-thickness with several gradient index values  $k$ , respectively. The impact of the plate thickness is noticeable on the critical buckling when ( $a/h < 10$ ). The critical buckling increasing as the side-to-thickness increases. As the plate gets thinner, there is no major changes in the critical buckling. In general, the critical buckling of thinner FG plate is higher than thick FG plate.

Figures 4 and 5 illustrate the dimensionless critical buckling under uniaxial and biaxial compression versus aspect ratio with several gradient index values  $k$ , respectively. The critical buckling escalates gradually as the aspect ratio increases. Moreover, uniaxial compression causes greater critical buckling than biaxial compression.

From Figures 2-5, it is obvious that the increasing of the gradient index  $k$  causes a reduction in the critical buckling. In addition, the critical buckling in case  $\epsilon_z \neq 0$  is slightly higher in comparison with  $\epsilon_z = 0$  because of normal strain effect on the plate. Moreover, the ceramic

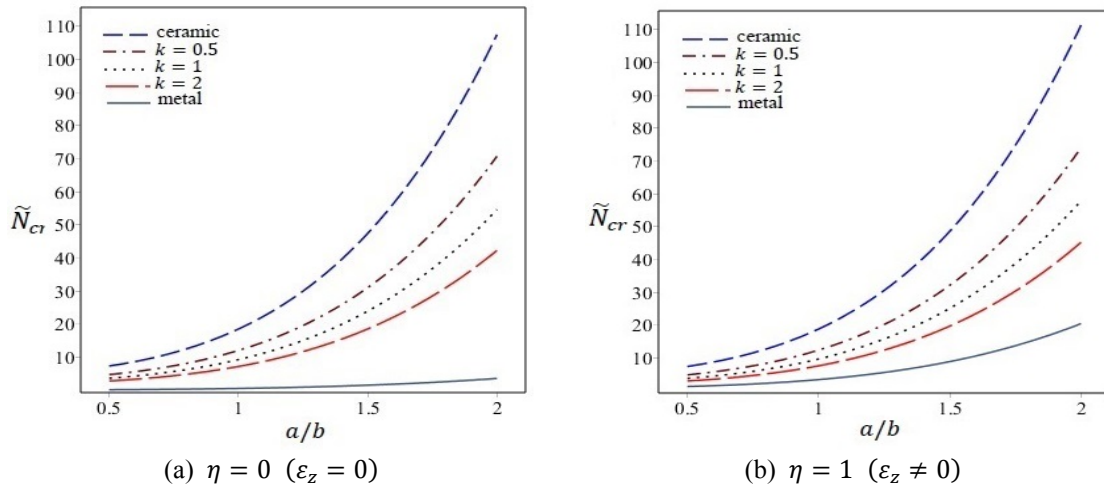


Fig. 4 The influence of aspect ratios ( $a/b$ ) on dimensionless critical buckling ( $\tilde{N}_{cr}$ ) of an FG plate under uniaxial compression for several gradient index ( $k$ ) when  $a/h = 10$

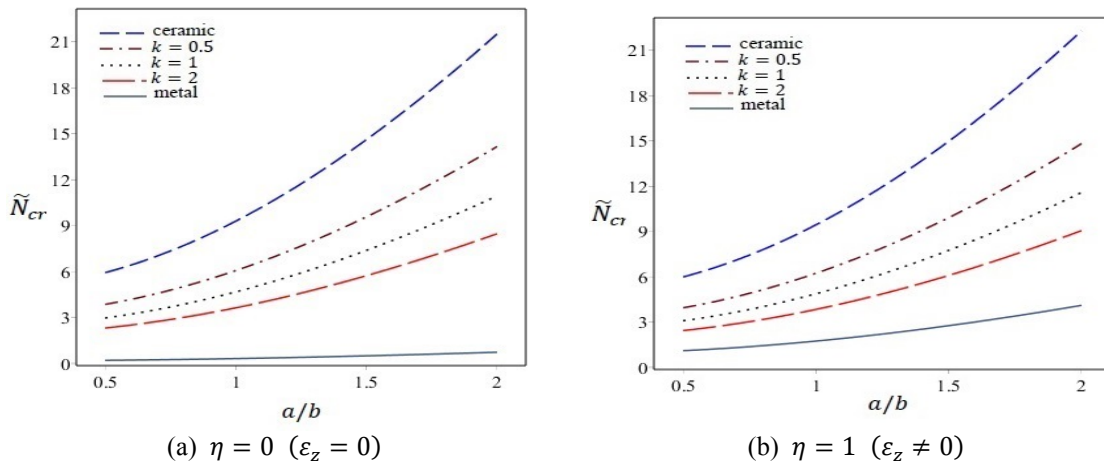


Fig. 5 The influence of aspect ratios ( $a/b$ ) on dimensionless critical buckling ( $\tilde{N}_{cr}$ ) of an FG plate under biaxial compression for several gradient index ( $k$ ) when  $a/h = 10$

surface has the highest critical buckling and the metal surface has the lowest and the critical buckling for the metal surface is higher when  $\varepsilon_z \neq 0$  compare to  $\varepsilon_z = 0$ . This approves that the normal strain effect depends on plate material. Furthermore, it is apparent that the critical buckling is higher under uniaxial loads than the critical buckling under biaxial compression.

## 6. Conclusions

The mechanical buckling analysis of a simply supported rectangular FG plate is examined. The analysis is achieved by employing a refined higher-order shear and normal deformation theory. The theory does not involve a shear correction coefficient. Navier's technique is applied to examine mechanical buckling of a simply-supported FG plate. The current results studied the

critical buckling exposed to uniaxial and biaxial compression loads. Furthermore, the influence of aspect ratio, side-to-thickness ratio, power law index and different loading conditions on the critical buckling are investigated. The numerical results of the mechanical critical buckling are compared with those obtained based on (Quasi-3D) by Thai and Choi (2012), (HSDT) by Reddy *et al.* (2013) and (HSDT) by Thinh *et al.* (2016). The results of the current theory are in excellent agreement considering the transverse normal effect. The current theory addresses the significant influence of the inclusion of normal strain on the critical buckling of thick and moderately thick FG plates. As its presented accurate estimation of the critical buckling load for thick plates compared to the other higher-order shear deformation plate theories with  $\varepsilon_z = 0$ . Moreover, the effect of FG material, plate structure and geometric parameters on the normal strain are presented. Therefore, the current results offer benchmark results. This can be beneficial for the interpretation of different plate theories as well compare the results achieved by other estimated approaches for instance the meshless method.

## References

- Birman, V. (1995), "Stability of functionally graded hybrid composite plates", *Compos. Eng.*, **5**(7), 913-921.
- Bodaghi, M. and Saidi, A.R. (2011), "Thermoelastic buckling behavior of thick functionally graded rectangular plates", *Arch. Appl. Mech.*, **81**(11), 1555-1572.
- Carrera, E. (2005), "Transverse normal strain effects on thermal stress analysis of homogeneous and layered plates", *ALAA J.*, **43**(10), 2232-2242.
- Fekrar, A., El Meiche, N., Bessaim, A., Tounsi, A. and Adda Bedia, E.A. (2012), "Buckling analysis of functionally graded hybrid composite plates using a new four variable refined plate theory", *Steel Compos. Struct.*, **13**(1), 91-107.
- Feldman, E. and Aboudi, J. (1997), "Buckling analysis of functionally graded plates subjected to uniaxial loading", *Compos. Struct.*, **38**(1-4), 29-36.
- Huang, Y. and Li, X.F. (2010), "Buckling of functionally graded circular columns including shear deformation", *Mater. Des.*, **31**(7), 3159-3166.
- Javaheri, R. and Eslami, M.R. (2011), "Thermal buckling of functionally graded plates based on higher order theory", *J. Therm. Stresses*, **25**(7), 603-625.
- Kiani, Y. and Eslami, M.R. (2010), "Thermal buckling analysis of functionally graded material beams", *Int. J. Mech. Mater. Des.*, **6**(3), 229-238.
- Kiani, Y. and Eslami, M.R. (2012), "Thermal buckling and post-buckling response of imperfect temperature-dependent sandwich FGM plates resting on elastic foundation", *Arch. Appl. Mech.*, **82**(7), 891-905.
- Lanhe, W. (2004), "Thermal buckling of a simply supported moderately thick rectangular FGM plate", *Compos. Struct.*, **64**(2), 211-218.
- Matsunaga, H. (2009), "Thermal buckling of functionally graded plates according to a 2D higher-order deformation theory", *Compos. Struct.*, **90**(1), 76-86.
- Mohammadi, M., Saidi, A. and Jomehzadeh, R.E. (2010), "A novel analytical approach for the buckling analysis of moderately thick functionally graded rectangular plates with two simply-supported opposite edges", *Proc. Inst. Mech. Engrs. Part C J. Mech. Eng. Sci.*, **224**(9), 1831-1841.
- Mokhtar, B., Abedlouahed, T., El Abba, A.B. and Abdelkader, M. (2009), "Buckling analysis of functionally graded plates with simply supported edges", *Leonardo J. Sci.*, **8**(15), 21-32.
- Mozafari, H. and Ayob, A. (2012), "Effect of thickness variation on the mechanical buckling load in plates made of functionally graded materials", *Proc. Tech.*, **1**, 496-504.
- Neves, A.M.A., Ferreira, A.J.M., Carrera, E., Cinefra, M., Roque, C.M.C., Jorge, R.M.N. and Soares, C.M.M. (2013), "Free vibration and buckling analysis of isotropic and sandwich functionally graded plates using a quasi-3D higher-order shear deformation theory and a meshless technique", *Compos. B*, **44**(1), 657-674.

- Reddy, B.S., Kumar, J.S., Reddy, C.E. and Reddy, K.V. (2013), "Buckling analysis of functionally graded material plates using higher order shear deformation theory", *J. Compos.*, **2013**, 1-12.
- Reddy, J.N. (1984), "A simple higher-order theory for laminated composite plates", *J. Appl. Mech.*, **51**(4), 745-752.
- Reddy, J.N. (1997), "Mechanics of laminated composite plate: Theory and analysis", CRC Press, New York, U.S.A.
- Saha, R. and Maiti, P.R. (2012), "Buckling of simply supported FGM plates under uniaxial load", *Int. J. Civil Struct. Eng.*, **2**(4), 1036-1050.
- Sepiani, H.A., Rastgoo, A., Ebrahimi, F. and Ghorbanpour Arani, A. (2010), "Vibration and buckling analysis of two-layered functionally graded cylindrical shell, considering the effects of transverse shear and rotary inertia", *Mater. Des.*, **31**(3), 1063-1069.
- Shariat, B.A.S. and Eslami, M.R. (2005), "Buckling of functionally graded plates under in plane compressive loading based on the first order plate theory", *Proceedings of 5th International Conference on Composite Science and Technology (ICCST/5)*, Sharjah, UAE, February.
- Shen, H.S. (2007), "Thermal post-buckling behavior of shear deformable FGM plates with temperature-dependent properties", *Int. J. Mech. Sci.*, **49**(4), 466-478.
- Thai, H.T. and Choi, D.H. (2012), "An efficient and simple refined theory for buckling analysis of functionally graded plates", *Appl. Math. Model.*, **36**(3), 1008-1022.
- Thai, H.T. and Vo, T.P. (2013), "A new sinusoidal shear deformation theory for bending, buckling, and vibration of functionally graded plates", *Appl. Math. Model.*, **37**(5), 3269-3281.
- Thinh, T.I., Tu, T.M., Quoc, T.H. and Long, N.V. (2016), "Vibration and buckling analysis of functionally graded plates using new eight-unknown higher order shear deformation theory", *Lat. Am. J. Solids Struct.*, **13**(3), 456-477.
- Yang, J., Liew, K.M. and Kitipornchai, S. (2005), "Second-order statistics of the elastic buckling of functionally graded rectangular plates", *Compos. Sci. Tech.*, **65**(7-8), 1165-1175.
- Zenkour, A.M. (2005), "A comprehensive analysis of functionally graded sandwich plates: Part 2 - Buckling and free vibration", *Int. J. Solids Struct.*, **42**(18-19), 5224-5242.
- Zenkour, A.M. (2006), "Generalized shear deformation theory for bending analysis of functionally graded plates", *Appl. Math. Model.*, **30**(1), 67-84.
- Zenkour, A.M. (2007), "Benchmark trigonometric and 3-D elasticity solutions for an exponentially graded thick rectangular plate", *Arch. Appl. Mech.*, **77**(4), 197-214.
- Zenkour, A.M. and Sobhy, M. (2010), "Thermal buckling of various types of FGM sandwich plates", *Compos. Struct.*, **93**(1), 93-102.
- Zhao, X., Lee, Y.Y. and Liew, K.M. (2009), "Mechanical and thermal buckling analysis of functionally graded plates", *Compos. Struct.*, **90**(2), 161-171.